Published in Superlattices and Microstructures 40, issues 4-6, 418-425, 2006
which should be used for any reference to this work

MBE growth of nitride-based photovoltaic intersubband detectors

E. Monroy[a], F. Guillot[a,*], S. Leconte[a], E. Bellet-Amalric[a], E. Baumann[b], F. Giorgetta[b], D. Hofstetter[b], L. Nevou[c], M. Tchernycheva[c], L. Doyennette[c], F.H. Julien[c], T. Remmele[d], M. Albrecht[d]

[a] *Equipe mixte CEA-CNRS-UJF Nanophysique et Semiconducteurs, DRFMC/SP2M/PSC, CEA-Grenoble, 17 rue des Martyrs, 38054 Grenoble cedex 9, France*
[b] *University of Neuchâtel, 2000 Neuchâtel, Switzerland*
[c] *Action OptoGaN, Institut d'Electronique Fondamentale, Université Paris-Sud, UMR 8622 CNRS, 91405 Orsay cedex, France*
[d] *Institut für Kristallzüchtung, Max-Born-Strasse 2, D-12489 Berlin, Germany*

Abstract

In this work, we present the plasma-assisted molecular-beam epitaxial growth of quantum well infrared photodetector (QWIP) structures, including the Si-doped GaN/AlN short-period superlattice of the active region, conductive AlGaN claddings and integration of the final device. The growth of Si-doped GaN/AlN multiple quantum well (QW) structures is optimized by controlling substrate temperature, metal excess and growth interruptions. Structural characterization confirms a reduction of the interface roughness to the monolayer scale. *P*-polarized intersubband absorption peaks covering the 1.33–1.91 μm wavelength range are measured on samples with QW thickness varying from 1 to 2.5 nm. The absorption exhibits Lorentzian shape with a line width around 100 meV in QWs doped 5×10^{19} cm^{-3}. To prevent partial depletion of the QWs owing to the internal electric field, we have developed highly-conductive Si-doped AlGaN cladding layers using In as a surfactant during growth. Complete ISB photodetectors with 40 periods of 1 nm-thick Si-doped GaN QWs with 2 nm-thick AlN barriers have been grown on conductive AlGaN claddings, the Al mole fraction of the cladding matching the average Al content of the active region. Temperature-dependent photovoltage measurements reveal a narrow (∼90 meV) detection peak at 1.39 μm.

Keywords: GaN; Superlattices; Intersubband; QWIP; Molecular-beam epitaxy

* Corresponding author. Tel.: +33 438784022.
E-mail address: fabien.guillot@cea.fr (F. Guillot).

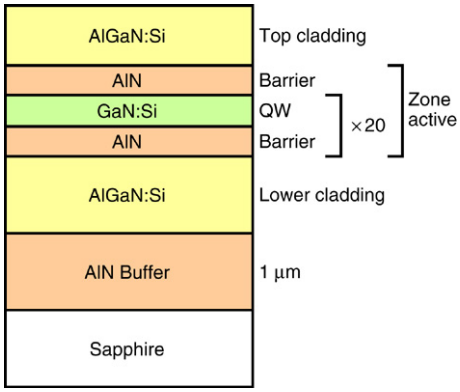

Fig. 1. Schematic structure of an AlGaN/AlN/GaN QWIP structure.

1. Introduction

Nitride semiconductors are promising candidates to develop high-bit-rate intersubband (ISB) devices operating at optical fiber telecommunication wavelengths (1.3 μm, 1.55 μm), owing to their large conduction band offset (∼2 eV in the GaN/AlN system) and subpicosecond scattering rates. ISB absorption in both QW [4,12,11,7,18] and quantum dot (QD) superlattices [14,17,6] has been demonstrated, and several prototypes of ISB detector have recently been reported [9,3, 10,19]. These developments are possible thanks to improved deposition techniques for AlGaN, GaN and AlN layers [13,16].

In this work we review our progress towards the fabrication of nitride-based ISB devices operating in the 1.3–1.55 μm range. We present the optimization of plasma-assisted MBE growth of quantum well infrared photodetector (QWIP) structures, including the Si-doped GaN/AlN short-period superlattice of the active region, AlGaN claddings and integration of the final device. Finally we discuss the structural, optical and electrical characterization of a complete QWIP.

2. Experimental

AlGaN/AlN/GaN multiple-quantum-well (MQW) structures have been synthesized by plasma-assisted molecular-beam epitaxy (PAMBE) on *c*-sapphire. The growth rate was fixed at ∼0.3 ML/s (=280 nm/h) by the flux of active nitrogen. The complete QWIP structure is presented in Fig. 1. One of the main issues to grow a nitride-based QWIP structure is strain management: Cracks and dislocations, which must be absolutely avoided, are the direct consequence of lattice-mismatch between the active region, claddings and substrate. All the devices synthesized were grown on a 1 μm-thick AlN buffer layer, in order to induce a compressive strain in the layers and hence prevent relaxation by cracking.

3. Results and discussion

3.1. Si-doped GaN/AlN multiple-quantum-well structures

The growth optimization of GaN/AlN interfaces requires determining conditions compatible for GaN and AlN growth, GaN being the most restrictive material owing to its lower decomposition temperature. Best GaN structural quality is achieved by depostion under Ga-rich

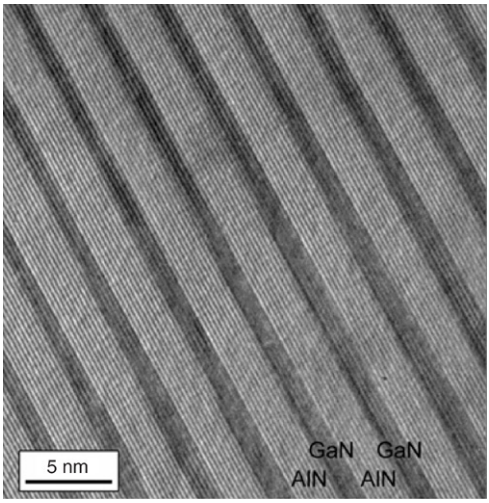

Fig. 2. HRTEM image of the active region of a QWIP structure.

conditions with two monolayers (2 ML) of Ga-excess segregating at the growth front [1]. The quality of the GaN/AlN heterostructures was found to be particularly sensitive to the Ga/N ratio. The strain fluctuations induced by Si doping and by the presence of the AlN barriers favor the formation of V-shaped pits, even in layers grown in the regime of 2 ML Ga-excess [15,8]. The suppression of these defects has been achieved by an enhancement of the Ga-flux so that growth is performed at the limit of Ga-accumulation.

In the case of AlN, Al-rich conditions are required to achieve two-dimensional growth. However, Al is not desorbed from the surface at standard growth temperatures for GaN. Therefore, to prevent Al accumulation at the surface, it is necessary to perform periodic growth interruptions under nitrogen. An alternative approach to prevent growth interruptions consists in using Ga as a surfactant for the growth of AlN, with the Al flux corresponding to the Al/N stoichiometry and using an additional Ga flux to stabilize the surface. Since the Al–N binding energy is much higher than the Ga–N binding energy, Ga segregates on the surface and is not incorporated into the AlN layer. Best interface roughness has been achieved by using Ga as a surfactant during the growth of AlN, without growth interruptions [16].

Conversely, we analyzed the effect of growth temperature on the quality of the GaN/AlN interfaces. It was observed that overgrowth of GaN QWs with AlN at high temperatures results in an irregular thinning of the QW thickness owing to exchange of Ga-atoms in the GaN layer with Al [5]. This is a thermally activated phenomenon that becomes relevant for AlN growth temperatures above 730 °C.

To conclude, best interface results were achieved at a substrate temperature $T_S = 720$ °C, growing AlN at the Al/N stoichiometry without growth interruptions and using also Ga as a surfactant during the growth of AlN barriers. Under these conditions, the samples present a flat surface morphology with an rms surface roughness of 1.0–1.5 nm measured in an area of 5×5 μm^2. Furthermore, high-resolution transmission electron microscopy (HRTEM) shows homogeneous QWs, with an interface roughness of ∼1 ML (see Fig. 2 and interface analysis in Ref. [16]).

The ISB absorption of a series of 20-period Si-doped AlN/GaN MQW structures with 2–3 nm AlN barriers and various GaN QW thicknesses was investigated using Fast Fourier Transform

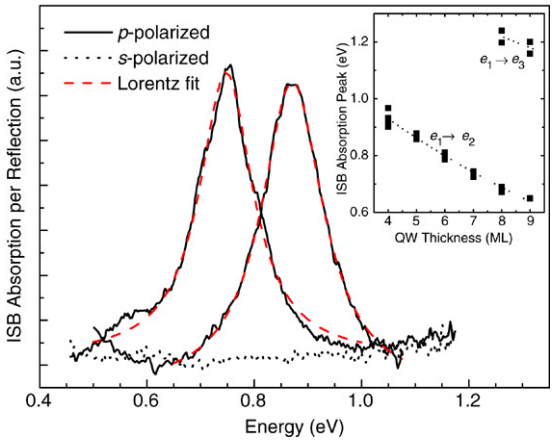

Fig. 3. Room-temperature ISB absorption spectra of AlN/GaN MQW structures for p-polarized and s-polarized light. The QW thicknesses are equal to 5 ML and 7 ML. Dashed lines present Lorentzian fits of the spectra. Inset: Variation of the $e_1 \rightarrow e_3$ and $e_1 \rightarrow e_3$ ISB absorption peaks as a function of the QW width, for samples doped in the QWs at 5×10^{19} cm^{-3}.

infrared spectroscopy [18]. The sample facets were polished at a 45° angle to form a multipass waveguide with 4–6 total internal reflections. The transmission for p-and s-polarized light was measured at room temperature using a deuterated triglycine sulfate photodetector. As an example, Fig. 4 shows the ISB absorption of Si-doped AlN/GaN MQWs with a QW thickness of 5 ML and 7 ML. The samples show a pronounced p-polarized absorption, attributed to transition from the first to the second electronic levels in the QW ($e_1 \rightarrow e_2$), while no absorption was found for s-polarized light within experimental accuracy. The spectra present a Lorentzian shape, indicative of homogeneous broadening of the absorption. The line width of the absorption remains in the 70–120 meV range for QWs doped at 5×10^{19} cm^{-2}, and the ISB absorption efficiency per reflection attains 3%–5%. A record bandwidth of ∼40 meV was achieved in non-intentionally doped structures. As displayed in the inset of Fig. 3, the ISB absorption peak can be tuned in the 1.33–1.91 μm wavelength range by changing the QW thickness from 4 to 10 ML. For larger QWs, the $e_1 \rightarrow e_3$ transition is observed [18]. This transition is allowed in nitride QWs because of the presence of a strong internal electric field in the well that breaks the symmetry of the potential. Detailed modeling of ISB absorption of these samples is presented in Ref. [18].

3.2. Growth of the AlGaN claddings

The QWIP cladding layers play an important role in the distribution of the internal electric field in the active region. Simulations of the band diagram using a self-consistent Schroedinger–Poisson equation solver show that the use of GaN claddings induces an electric field at the active region, which results in the accumulation of a two-dimensional electron gas (2DEG) at the interface between the active region and the bottom cladding, and a depletion region that overlaps partly with the top cladding and several periods of the active region (see Fig. 4). This electric field is mostly due to the difference between the spontaneous polarization of the claddings and the average spontaneous polarization of the active region. The electric field at the active region can be attenuated by using AlGaN as a cladding layer, with an Al mole fraction corresponding to the average Al content of the active region. This design is also advisable in

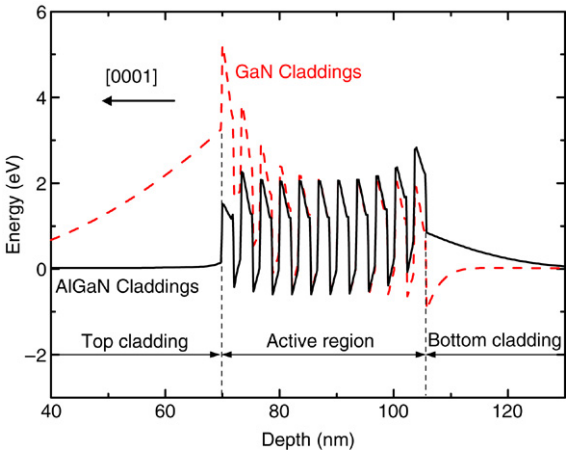

Fig. 4. Band diagram of a 10-period GaN/AlN QWIP structure with GaN and AlGaN claddings.

order to achieve a uniform strain distribution along the active region and reduce the formation of misfit dislocations.

However, there are intrinsic difficulties in growing high-quality AlGaN alloys, since the strength of the Al–N bond results in a reduction of the surface mobility of Al as compared to Ga species in PAMBE. The growth of AlGaN layers with an Al mole fraction lower than 35% can be performed under Ga-rich conditions without deterioration of the surface morphology or crystalline quality. However, when increasing the Al mole fraction to values higher than 50%, we observe a significant enhancement of the surface roughness, to typical rms values of ∼4 nm on a surface of 5×5 μm^2. In a previous work, we demonstrated the capability of In as a surfactant for AlGaN growth, delimiting the range of substrate temperatures and In fluxes at which an In adlayer is dynamically-stable on $Al_xGa_{1-x}N$ (0001) [13]. In the present work, we applied this growth procedure to the QWIP cladding layers, achieving a reduction of the surface roughness (<3 nm rms on a $Al_{0.6}Ga_{0.4}N$ surface of 5×5 μm^2), and an improvement in the crystalline quality of the samples, as measured by high-resolution X-ray diffraction (typical values of the full width at half maximum (FWHM) of the (0002) ω-scan around 400″).

Alternatively, highly-conductive claddings are required to reduce the series resistance of the devices and hence enhance their operation bandwidth. We succeeded in synthesizing low-resistivity Si-doped $Al_{0.6}Ga_{0.4}N$ layers. Resistivities as low as 0.01 Ω cm are achievable with carrier concentrations larger than 10^{19} cm^{-3}, as illustrated in Fig. 5. The activation energy of Si donors measured by Hall in samples with different Si concentration decreases from ∼190 meV in non-intentionally doped samples to 15 meV for $n = 2 \times 10^{19}$ cm^{-3}. No effect of Si on the structural quality is observed by AFM or HRXRD.

3.3. Characterization of complete devices

The QWIP structure under study consists of 40 periods of 1.0 nm-thick Si-doped GaN QWs with 2.0 nm-thick AlN barriers, grown on 1 μm-thick AlN-on-sapphire substrates. The doping level in the GaN QWs was 1×10^{19} cm^{-3}. Prior to the growth of the active region, a 250 nm thick Si-doped $Al_{0.65}Ga_{0.35}N$ buffer layer was deposited. On top of the active region, we deposited a Si-doped $Al_{0.65}Ga_{0.35}N$ cap layer, with a thickness of 5 nm. Fig. 6 presents an AFM scan of the

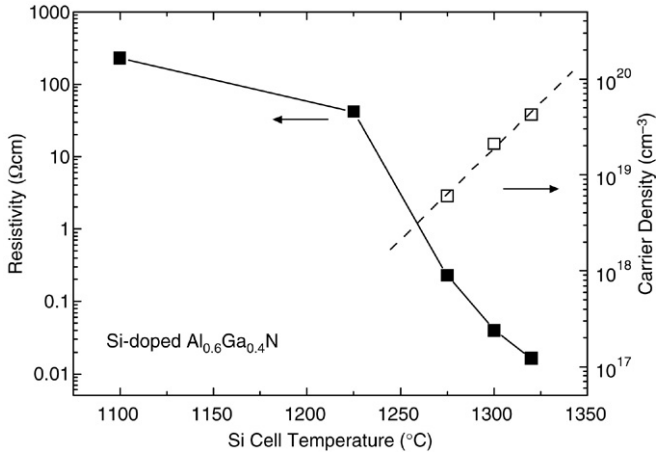

Fig. 5. Variation of the resistivity and carrier concentration of a 500 nm thick Si-doped $Al_{0.6}Ga_{0.4}N$ layer as a function of the Si cell temperature.

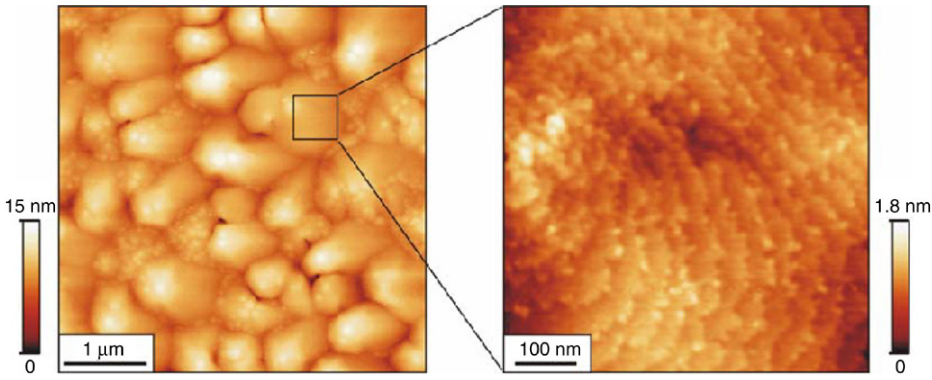

Fig. 6. AFM surface scans of a complete AlGaN/AlN/GaN QWIP structure as described in Fig. 1, with an $Al_{0.35}Ga_{0.35}N$ top cladding of 5 nm. The rms roughness on the 5×5 µm^2 image is 1.7 nm. In the zoomed image on the right side, we observe the atomic-step terraces typical for the growth of GaN, indicating a short-range roughness at the monolayer scale.

sample, showing an rms surface roughness of about 1.7 nm on an area 5×5 µm^2. In the zoomed image of Fig. 6, we observe atomic-step terraces, which indicate a short-range roughness at the monolayer scale.

The structural quality of the QWIP structure was further assessed by HRXRD. Fig. 7 shows the (θ–2θ)-scan of the (0002) X-ray reflection, displaying superlattice satellite peaks up to the second order, which confirm an average period of 2.93 nm. From simulations of this scan (also presented in Fig. 7), and from the (10–15) reciprocal space map, we verified that the average Al mole fraction of the claddings matches the average Al content of the MQW structure, and that the whole structure is strained on the AlN buffer layer.

To fabricate the QWIP, the above-described sample was polished in a standard multipass geometry with a mirror-like back and two parallel 45° wedges. Two Cr/Au (10/400 nm) ohmic contacts were deposited on the sample surface, separated by 3 mm. In between, a large stripe

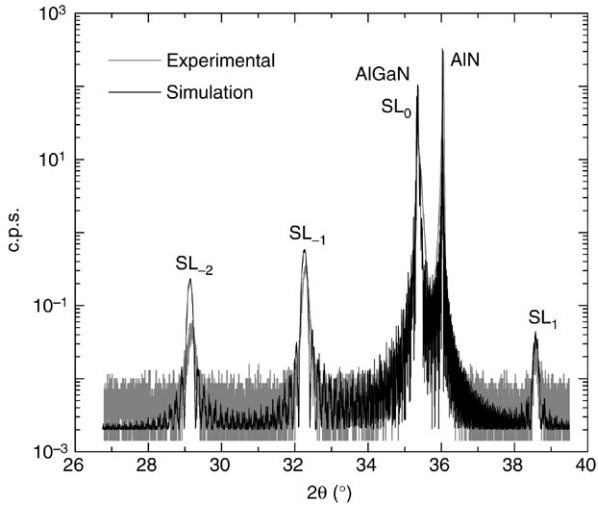

Fig. 7. HRXRD θ–2θ scan of the (0002) reflection of a QWIP structure. Superlattice satellite peaks up to the second order are clearly visible, whereas the superlattice zero-order reflection peak (SL_0) overlaps with the $Al_{0.65}Ga_{0.35}N$ reflection. An average period of 2.93 nm is obtained from the intersatellite distance. The simulation was performed using the program X'Pert Epitaxy 40 from Phillips Analytical, assuming that the structure is fully strained on the AlN buffer.

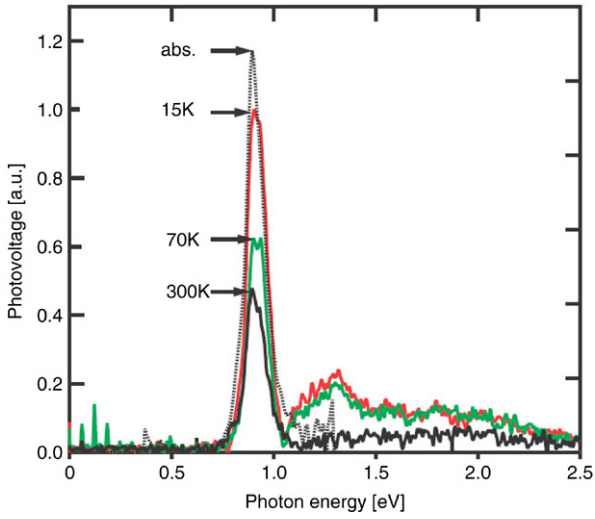

Fig. 8. Temperature-dependent photovoltage measurements for p-polarized light. The absorbance spectrum is shown as a dashed line for comparison.

of the same contact metals was evaporated on top of a 50 nm thick SiO_2 layer deposited on the semiconductor surface. Fig. 8 presents the characterization of this device as a photovoltaic ISB photodetector. In this experiment, the sample was illuminated by the white light source of the Fourier spectrometer. Similarly as described earlier in Ref. [2], the Schottky contact leads to a band bending at the sample surface, depleting several periods of the active region. Illumination results in a photovoltage, which can be observed at up to room temperature, as shown in Fig. 8.

A good agreement between the photovoltage signal and the absorbance peak is evident. The photovoltage at 10 K peaks at 0.915 eV (1.39 μm), and has a FWHM of 90 meV. This extremely narrow peak confirms the good structural material quality.

4. Conclusions

PAMBE has been adapted for the growth of AlGaN/AlN/GaN QWIPs operating in the optical-fiber telecommunication spectral range. Si-doped GaN/AlN multiple QW structures with interface roughness at the monolayer scale were successfully synthesized. These structures present ISB absorption peaks that can be tuned in the 1.33–1.91 μm wavelength range by varying the QW thickness from 1 to 2.5 nm. To prevent partial depletion of the QWs owing to the internal electric field, we have developed highly-conductive Si-doped AlGaN cladding layers using In as a surfactant during growth. Complete ISB photovoltaic detectors have been fabricated. Temperature-dependent photovoltage measurements reveal a narrow (∼90 meV) detection peak at 1.39 μm.

Acknowledgment

This work is supported by the 6th European Framework Program within the project NITWAVE (STREP 004170).

References

[1] C. Adelmann, J. Brault, G. Mula, B. Daudin, L. Lymperakis, J. Neugebauer, Phys. Rev. B 67 (2003) 165419.
[2] E. Baumann, F.R. Giorgetta, D. Hofstetter, H. Lu, X. Chen, W.J. Schaff, L.F. Eastman, S. Golka, W. Schrenk, G. Strasser, Appl. Phys. Lett. 87 (2005) 191102.
[3] L. Doyennette, L. Nevou, M. Tchernycheva, A. Lupu, F. Guillot, E. Monroy, R. Colombelli, F.H. Julien, Electron. Lett. 41 (2005) 1077.
[4] C. Gmachl, H.M. Ng, A.Y. Cho, Appl. Phys. Lett. 79 (2001) 1590.
[5] N. Gogneau, F. Fossard, E. Monroy, S. Monnoye, H. Mank, B. Daudin, Appl. Phys. Lett. 84 (2004) 4224.
[6] F. Guillot, E. Bellet-Amalric, E. Monroy, M. Tchernycheva, L. Nevou, L. Doyennette, F.H. Julien, Le Si Dang, T. Remmele, M. Albrecht, T. Shibata, M. Tanaka, J. Appl. Phys. 100 (2006) 044326.
[7] A. Helman, M. Tchernycheva, A. Lusson, E. Warde, F.H. Julien, Kh. Moumanis, G. Fishman, E. Monroy, B. Daudin, D.Le Si Dang, E. Bellet-Amalric, D. Jalabert, Appl. Phys. Lett. 83 (2003) 5196.
[8] M. Hermann, E. Monroy, A. Helman, B. Baur, M. Albrecht, B. Daudin, O. Ambacher, M. Stutzmann, M. Eickhoff, Phys. Status Solidi c 1 (2004) 2210.
[9] D. Hofstetter, S.-S. Schad, H. Wu, W.J. Schaff, L.F. Eastman, Appl. Phys. Lett. 83 (2003) 572.
[10] D. Hofstetter, E. Baumann, F.R. Giorgetta, M. Graf, M. Maier, F. Guillot, E. Bellet-Amalric, E. Monroy, Appl. Phys. Lett. 88 (2006) 121112.
[11] N. Iizuka, K. Kaneko, N. Suzuki, Appl. Phys. Lett. 81 (2002) 1803.
[12] K. Kishino, A. Kikuchi, H. Kanazawa, T. Tachibana, Appl. Phys. Lett. 81 (2002) 1234.
[13] E. Monroy, B. Daudin, E. Bellet-Amalric, N. Gogneau, D. Jalabert, F. Enjalbert, J. Brault, J. Barjon, Le Si Dang, J. Appl. Phys. 93 (2003) 1550.
[14] K. Moumanis, A. Helman, F. Fossard, M. Tchernycheva, A. Lusson, F.H. Julien, B. Damilano, N. Grandjean, J. Massies, Appl. Phys. Lett. 82 (2003) 868.
[15] T. Nakamura, S. Mochizuki, S. Terao, T. Sano, M. Iwaya, S. Kamiyama, H. Amano, I. Akasaki, J. Cryst. Growth 237–239 (2002) 1129.
[16] E. Sarigiannidou, E. Monroy, N. Gogneau, G. Radtke, P. Bayle-Guillemaud, E. Bellet-Amalric, B. Daudin, J.L. Rouvière, Semicond. Sci. Technol. 21 (2006) 912.
[17] M. Tchernycheva, L. Nevou, L. Doyennette, A. Helman, R. Colombelli, F.H. Julien, F. Guillot, E. Monroy, T. Shibata, M. Tanaka, Appl. Phys. Lett. 87 (2005) 101912.
[18] M. Tchernycheva, L. Nevou, L. Doyennette, F.H. Julien, E. Warde, F. Guillot, E. Monroy, E. Bellet-Amalric, T. Remmele, M. Albrecht, Phys. Rev. B 73 (2006) 125347.
[19] A. Vardi, N. Akopian, G. Bahir, L. Doyennette, M. Tchernycheva, L. Nevou, F.H. Julien, F. Guillot, E. Monroy, Appl. Phys. Lett. 88 (2006) 143101.